Heliyon 10 (2024) e30178

Contents lists available at ScienceDirect

Heliyon

journal homepage: www.cell.com/heliyon

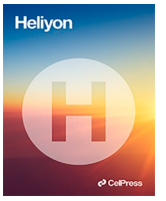

Research article

Multi-functional copper oxide nanoparticles synthesized using *Lagerstroemia indica* leaf extracts and their applications

Addisie Geremew [a], Lenaye Palmer [a], Andre Johnson [a], Sheena Reeves [b], Nigel Brooks [b], Laura Carson [a,*]

[a] *Cooperative Agricultural Research Center, Prairie View A&M University, Prairie View, TX, 77446, USA*
[b] *Department of Chemical Engineering, College of Engineering, Prairie View A&M University, Prairie View, TX, 77446, USA*

ARTICLE INFO

Keywords:
Copper oxide nanoparticles
Lagerstroemia indica, antimicrobial
Antioxidant
Seed germination
Wastewater treatment
Photodegradation

ABSTRACT

Developing multifunctional nanomaterials through environmentally friendly and efficient approaches is a pivotal focus in nanotechnology. This study aimed to employ a biogenic method to synthesize multifunctional copper oxide nanoparticles (LI-CuO NPs) with diverse capabilities, including antibacterial, antioxidant, and seed priming properties, as well as photocatalytic organic dye degradation and wastewater treatment potentials using *Lagerstroemia indica* leaf extract. The synthesized LI-CuO NPs were extensively characterized using UV–vis spectroscopy, dynamic light scattering (DLS), X-ray diffraction (XRD), scanning electron microscopy with energy dispersive X-ray spectroscopy (SEM-EDX), transmission electron microscopy (TEM), X-ray photoelectron spectroscopy (XPS), and Fourier transform-infrared spectroscopy (FT-IR). The colloid displayed surface plasmon resonance peaks at 320 nm, characteristic of LI-CuO NPs. DLS analysis revealed an average particle size of 93.5 nm and a negative zeta potential of −20.3 mV. FTIR and XPS analyses demonstrated that LI-CuO NPs possessed abundant functional groups that acted as stabilizing agents. XRD analysis indicated pure crystalline and spherical LI-CuO NPs measuring 36 nm in size. Antibacterial tests exhibited significant differential activity of LI-CuO NPs against both gram-negative (*Escherichia coli*, *Salmonella typhimurium*) and gram-positive (*Staphylococcus aureus* and *Listeria monocytogenes*) bacteria. In antioxidant tests, the LI-CuO NPs demonstrated a remarkable radical scavenging activity of 97.6 % at a concentration of 400 μg mL^{-1}. These nanoparticles were also found to enhance mustard seed germination at low concentrations. With a remarkable reusability, LI-CuO NPs exhibited excellent photocatalytic performance, with a degradation efficiency of 97.6 % at 150 μg/mL as well as a 95.6 % reduction in turbidity when applied to wastewater treatment. In conclusion, this study presents environmentally friendly method for the facile synthesis of LI-CuO NPs that could potentially offer promising applications in biomedicine, agriculture, and environmental remediation due to their multifunctional properties.

1. Introduction

The rapidly changing global climate and land degradation have posed significant challenges to sustainable agricultural production,

* Corresponding author.
E-mail address: lecarson@pvamu.edu (L. Carson).

https://doi.org/10.1016/j.heliyon.2024.e30178
Received 6 July 2023; Received in revised form 19 April 2024; Accepted 22 April 2024
Available online 30 April 2024

food safety, and the emergence of drug-resistant pathogens [1–4]. To address these multifaceted issues, the application of nanotechnology has gained substantial importance [5]. Nanotechnology offers the potential to mitigate agricultural losses, enhance food safety, combat drug-resistant pathogens, and address environmental pollution through waste and water treatments [6–10]. The burgeoning enthusiasm for nanomaterials research is intricately tied to their distinct characteristics, such as heightened reactivity, exceptional durability, significant surface-area-to-volume ratio, vast biological activity, and a plethora of other attributes [3,4,7,11–15].

The synthesis and use of metal oxide nanoparticles such as ZnO, CoO, TiO_2, Fe_2O_3, SnO_2, Bi_2O_3 and CuO have been studied for their environmental, agricultural, and biomedical applications than their metallic form [7,14],[16-23]. Due to their wider range of applications, there is a growing interest in the biofabrication of Copper oxide nanoparticles (CuO NPs). These applications encompass their efficacy as antimicrobial, antioxidant, and anticancer agents [7,14,16–18], as well as their utility in drug delivery mechanisms [7]. Additionally, CuO NPs play pivotal roles in waste treatment processes [15], pesticide formulations [13,14], and serve as integral components in nanosensor technology [24]. Furthermore, they exhibit prowess as photocatalysts [25], contributing significantly to thermal conductivity and energy storage systems [7,14,26]. Several physical and chemical methodologies have been documented for synthesizing CuO NPs [27–36]. However, these traditional synthesis methods are energy-intensive, expensive, and environmentally unfriendly [7,14,37]. To overcome these limitations, there exists a compelling need for adopting environmentally friendly and cost-effective synthesis approaches [4,37].

One promising avenue in green synthesis involves the use of natural materials including extracts from plants, microbes, and algae as potential reductant [6,37]. Plant extracts, in particular, provide an economically viable and environmentally friendly approach [4,37], harnessing the rich variety of phytomolecules including flavonoids, terpenes, alkaloids, vitamins, acids, tannins, phenols and many more metabolites they contain [4,6]. These phytochemicals demonstrate exceptional capabilities as reducing, stabilizing, and capping agents, facilitating precise control of nanoparticle size and shape [4,6,15,38]. CuO NPs have been successfully synthesized utilizing extracts sourced from diverse plant species such as *Bauhinia tomentosa* [7], *Brassica oleracea* [14], *Calotropis procera* [39], *Azadirachta indica* [40], *Albizia lebbeck* [41], *Catha edulis* [42]; *Capparis spinosa* [15], *Psidium guajava* [43], *Drypetes sepiaria* [44], *Syzygium alternifolium* [45], *Populus ciliata* [46], *Ruellia tuberosa* [43], and *Nerium oleander* [47]. While various plants have been employed for CuO NP synthesis, most studies have focused on single functionalities, overlooking the potential for multi-functional nanoparticles [48–50].

In this context, the Indian Crape myrtle (*Lagerstroemia indica* L.) is one of the most ecologically and ethnobotanically significant species endemic to China and introduced into other parts of the world [51,52]. The species is recognized for its substantial nutraceutical properties [53–56]. Nuclear magnetic resonance analysis showed that *L. indica* leaf contains a notable amount of gallic acid, 3-O-methylgallate, tellimagrandin, isovitexin, luteolin, brevifolin, vitexin, iso-orientin, orientin, astragalin, nilocitin, catechin, epicatechin, rutin, 2,3-hexahydroxydiphenic acid-α/β-glucoside, apigenin-7-*O-4C1*-β-D-glucoside, kaempferol, decarboxy ellagic acid and quercetin [53,56–58]. Thus, these diverse bioactive compounds make *L. indica* an ideal choice for nanoparticle synthesis. Several studies have examined the impact of biosynthesized silver nanoparticles on altering bacterial biofilms in both gram-negative and gram-positive bacteria [59], as well as investigating the anticancer, antimicrobial, and hemolytic properties of zinc oxide nanoparticles [60], using leaf extracts from *L. indica*. However, the potential of employing *L. indica* leaf extract in the synthesis of CuO NPs with multiple functionalities remains unexplored.

This study aimed to synthesize multifunctional CuO NPs for versatile applications in agriculture, biology, and the environment. To achieve this objective, a novel and environmentally friendly synthesis of CuO NPs was conducted using *L. indica* leaf extracts. This marks the pioneering use of *L. indica* leaf extracts for this purpose, as the green-synthesized CuO NPs underwent thorough characterization, evaluating their size, stability, crystallinity, purity, morphology, structural features, and chemical composition. Various analytical techniques, including UV–Vis spectrometry, X-ray diffraction (XRD), Fourier transform infrared spectroscopy (FTIR), and scanning electron microscopy with energy dispersive x-ray spectroscopy (SEM-EDX) analysis, were employed for this purpose. The study also explored the antioxidant and antimicrobial properties, photocatalytic dye degradation and wastewater treatment and seed priming efficacies of the synthesized CuO NPs. The findings contribute profound insights into the multifaceted capabilities of the synthesized CuO NPs, underscoring their pivotal role in addressing challenges across agricultural, biological, and environmental domains.

2. Materials and methods

2.1. Plant and chemicals

The leaves of *Lagerstroemia indica* were collected from the Prairie View A&M University (PVAMU) main campus, TX, USA in June 2, 0222. Subsequently, the sample underwent identification by the plant systematist at PVAMU. The voucher plant specimen (LITXUS-1072022) was deposited. Copper sulfate pentahydrate ($CuSO_4 \cdot 5H_2O$, 99.98 %), 1, 1-diphenyl-2-picryl hydrazyl (DPPH), ascorbic acid, methylene blue, methanol, ethanol, Trypticase Soy Broth (TSB) and Trypticase Soy Agar (TSA) were procured from Sigma–Aldrich (St. Louis, MO, USA). All chemicals, meticulously sourced as analytical grade, were used without additional purification.

2.2. Preparation of Lagerstroemia indica leaf extract

The aqueous leaf extract of *L. indica* was prepared with a slight modification of the method in our previous study [6]. Healthy leaves were first washed thoroughly with tap water to eliminate debris, followed by freeze-drying and grinding into powder using an

electrical blender. For aqueous extraction, 15 g of finely powdered sample was weighed and transferred to a 1L flask. Then 700 mL of distilled water was added and the mixture was sonicated under ultrasonic bath (Bransonic® MH-series, CPX-952-217R) for 90 min at 55 °C. The mixture was shaked for 72 h with an orbital shaker (IKA Basic Variable-Speed Digital Orbital Shaker, model, 115V) set to 300 rpm at 20 °C. The resulting solution was further filtered using polyvinylidene fluoride syringe filter with a pore size of 0.45 μm. The filtrate was stored at 4 °C pending the synthesis of CuO NPs.

2.3. Biosynthesis of CuO nanoparticles

Copper oxide nanoparticles (CuO NPs) were synthesized with slight modification of the method described by Alhalili [61]. In this approach, 10 mL of the pre-prepared leaf extract with a pH adjusted to 8.1 was combined with 90 mL of a 1 mM concentrated $CuSO_4{\cdot}5H_2O$ solution. The mixture, with its pH readjusted to 8.2, was stirred at 25 °C for 6 h until in a noticeable color change to black suspension observed. The mixture was then centrifuged at 20,000 rpm for 20 min, washed with deionized water, and dried at 80 °C for 4 h in an oven. The dried pellet was subjected to calcination in a furnace at 500 °C for 3 h to achieve stable CuO NPs. Afterward, the dried powder was washed with ethanol and centrifuged at 10,000 rpm for 20 min three times and the pellet was dried. Finally, the synthesized nanoparticles designated as LI-CuO NPs were stored in a glass ampoule within a desiccator until further characterization.

2.4. Characterization of biosynthesis of CuO NPs

The reduction of copper ions to LI-CuO NPs was firstly evaluated visually by inspecting color change. UV–Vis spectrophotometer (SpectraMax® PLUS 384) was employed to further monitor and confirm the formation of LI-CuO NPs in the absorption spectra ranged from 200 to 800 nm. Dynamic light scattering (DLS) was employed to determine the average particle size and distribution, polydispersity index (PDI) and zeta potential of the biosynthesized LI-CuO NPs with Litesizer™ 500 (Anton Paar, Austria). The numbers of measurements for these parameters were evaluated and enhanced by the Kalliope 3.2.5 (Anton Paar, Austria). To characterize the functional groups of phytochemicals serving as reducing and stabilizing agents, FTIR spectra of LILE and LI-CuO NPs were acquired using a JASCO/FTIR-6300 spectrophotometer, covering the range of 4000–500 cm^{-1} with a resolution of 4 cm^{-1} via the KBr disc technique. The synthesized LI-CuO nanoparticles were characterized using scanning electron microscopy (SEM) coupled with energy-dispersive X-ray spectroscopy (EDX) to analyze their morphological and elemental composition. Additionally, transmission electron microscopy (TEM) analysis was performed using a JEOL-2100+ High-Resolution TEM equipped with selected area electron diffraction (SAED) at 200 kV. The chemical composition of LI-CuO NPs was analyzed by X-ray photoelectron spectroscopy XPS (PHI 5000VersaProbeII, ULVAC-PHI Inc.) analyzer. Moreover, the crystallinity of the nanoparticles was taken by a powder diffractometer (XRD-7000, Shimadzu, Japan), operating at 40 kV and 30 mA, with Kα radiation ($\lambda = 1.54$ Å) in the range of $2\theta = 10° - 80°$. The average crystallite size (D) of LI-CuO NPs was computed using Debye-Scherrer's formula [62] given by equation (1):

$$D = k\,\lambda / \beta \mathrm{Cos}\theta \quad (1)$$

where θ is Bragg angle, β is the full width at half maximum (FWHM), k is shape factor ($k = 0.94$ in this work) and λ is the wavelength of incident X-rays ($\lambda = 1.54$ nm).

2.5. Antibacterial activity

An in vitro antibacterial activity of the LI-CuO NPs was assessed against different pathogenic bacteria including *Escherichia coli* 0157: H7, *Salmonella typhimurium* (ATCC 14028), *Staphylococcus aureus* (ATCC 12228), and *Listeria monocytogenes* (ATCC 19111) by the agar well diffusion method. The test microbes were cultured on TSB media and transferred to TSA plates, sub-cultured and incubated at 37 ± 2 °C for 24 h. Following the incubation, a colony was taken by sterilized swap and evenly smeared across the surface of TSA plate. The solid medium was softly punctured to make wells with diameter of 6 mm at equidistant. Then, 100 μL of 50, 75 and 100 μgmL^{-1} of synthesized LI-CuO NPs colloidal solutions and LILE (100 μgmL^{-1}) each were placed to wells and then incubated at 37 ± 2 °C for 24 h. The streptomycin (100 μgmL^{-1}) was used as a control. After incubation, inhibition zones (in millimeters) were measured using ProtoCOL3 (Synbiosis, Cambridge, UK).

2.6. Determination of minimum inhibitory and bactericidal concentrations

Initially, bacterial growth was adjusted to a density of 0.5 McFarland turbidity standard (A600 = 0.1), equivalent to 1×10^6 CFU/mL through serial dilutions in TSB media. Different concentrations of LI-CuO NPs ranging from 30 to 160 μg mL^{-1} in 10-unit intervals were prepared using sterilized water. Subsequently, bacterial culture (20 μL each strain) was mixed with each LI-CuO NP (80 μL) concentration and smeared on TSA plates. The plates were then incubated at 37 ± 2 °C for 24 h. For each dilution, a negative control comprising 80 μL of LI-CuO NPs and TSA (without bacterial inoculum) was used, while untreated bacteria in TSA medium served as the positive control. The minimum inhibitory concentration (MIC) was determined for each pathogenic bacterium as the lowest concentration at which full inhibition of bacterial growth occurred without cell killing. Additionally, the minimum bactericidal concentration (MBC) of LI-CuO NPs was assessed by subculturing bacteria with a concentration equal to or higher than MIC on TSA plates. The MBC value was defined as the lowest concentration at which no bacterial growth was observed. All experiments were conducted in triplicate.

2.7. Antioxidant activity of LI-CuO nanoparticles

The 2, 2- diphenyl-1-picrylhydrazyl (DPPH) assay was used to evaluate the relative free radical scavenging activity of the LILE, LI-CuO NPs, and the standard (ascorbic acid) following the method by Geremew et al. [6]. About 30 μL of different concentrations (25, 50, 100, 200, 300 and 400 μg mL^{-1}) of LILE, ascorbic acid and LI_CuO NPs each were mixed with 170 μL of DPPH radical solution (0.1 mM in methanol) in a 96-well microplate. After 30 min of incubation in darkness, absorbance was measured at 517 nm using a UV–Vis spectrophotometer (SpectraMax® PLUS 384), with negative control (DPPH methanol reagent without extract and LI-CuO NPs) and positive control (ascorbic acid with DPPH). Percentage inhibition was calculated following our previous protocol [6].

2.8. Seed germination experiment

Mustard (*Brassica juncea* L. *Czern*) was selected as a model plant to assess the impact of LI-CuO NPs on germination rate. Seeds of *B. juncea* were obtained from Twilley Seed Company (Hodges, SC, USA), sterilized in 10 % (v/v) $NaClO_4$ solution for 10 min, and thoroughly rinsed with sterilized deionized water. Once rinsed, seeds were immersed in LI-CuO NPs solution of varying concentrations (0, 50, 100, 150 and 200 mg L^{-1}) for 5 min. Twenty-five seeds were evenly placed onto each Petri dish lined with filter paper. Then 5 mL of either deionized water (control) or the respective concentrations of LI-CuO NPs solution were poured into each dish. Each treatment was triplicated. The tightly sealed Petri dishes were kept at 25 °C until germination occurred. After 5 days, the seed germination rate (GR) was estimated by computing the proportion of seeds that had germinated. Also, relative seed germination inhibition (RGI) was calculated [63] using equation (2):

$$RGI\ (\%) = [(GR_{control}\_GR_{treat})/(GR_{control})]\ X\ 100 \quad (2)$$

2.9. Photocatalytic dye degradation efficiency of LI-CuO NPs and reusability

The photocatalytic efficiency of biosynthesized LI-CuO NPs was assessed by degrading methylene blue (MB) in aqueous solution under sunlight, following methods adapted from Sukumar et al. [64]. MB solution (100 μg/mL) was prepared by dissolving 1 mg in 10 mL of deionized water under aseptic conditions. Different concentrations of LI-CuO NPs (5, 10, 25, 50, 100 and 150 μg/mL) were prepared from a 500 μg/mL stock solution. From each concentration of the synthesized LI-CuO NPs 10 mL was added to 100 mL of MB samples. MB solution without the addition of LI-CuO NPs was used as control. To maintain the adsorption-desorption balance between LI-CuO NPs and MB, the mixture was stirred in dark for 5 min before irradiation. The reaction solution was then kept exposed to direct sunlight irradiation. During the course of photocatalysis 3 mL of sample solution were taken at the interval of 30 min and centrifuged at 10, 000 RPM for 15 min. Then supernatants were obtained to determine rate and efficiency of MB degradation by measuring absorbance at 664 nm using UV–Vis spectrophotometer (SpectraMax® PLUS 384). The photocatalytic activity measurement period ranged from 0 to 150 min. Percent dye degradation was computed [65] as indicated in equation (3):

$$Degradation\ (\%) = [(C_0\text{-}C_t)/(C_0)]\ X\ 100 \quad (3)$$

where, C_0 and C_t represent absorbances at the 0^{th} and tth minutes, respectively.

For further large-scale photocatalytic applications, the reusability of LI-CuO NPs was assessed over five cycles using a maximum concentration of LI-CuO NPs of 150 μg/mL employed in MB degradation. Following the first cycle, the nano-catalyst was washed three times with distilled water and then dried at 50 °C in an oven to eliminate any residual water prior to applying in the second cycle.

2.10. Potential of LI-CuO NPs in wastewater treatment

Wastewater samples released from the animal production site at Prairie View A&M University main campus, TX, USA were collected and homogenized following proper aseptic conditions. The initial turbidity of the wastewater was measured using a turbidimeter (Oakton T-100). Coagulation/flocculation/sedimentation (CFS) assay was conducted to assess the application of LI-CuO NPs in wastewater treatment. About 10 mL of LI-CuO NPs of different concentrations (10, 25, 50, 100 and 150 mg L^{-1}) were added to 100 mL of the wastewater. Wastewater without LI-CuO NPs was used as a control. A combination of rapid mixing at 150 rpm for 4 min followed by slow mixing at 50 rpm for 15 min, and coupled with 90 min of sedimentation was carried out. After sedimentation, samples were taken from the supernatant for turbidity measurements using a turbidimeter (Oakton T-100). From the initial turbidity (TI) and final turbidity (TF) measurements, the turbid removal efficiency of LI-CuO NPs was estimated using equation (4):

$$Turbidity\ removal\ (\%) = [(TI\text{-}\ TF)/(TI)]\ x\ 100. \quad (4)$$

2.11. Statistical analysis

Antioxidant, antimicrobial activities, relative germination inhibition, and dye degradation efficiency data across LI-CuO NPs concentrations underwent one-way ANOVA analysis using the agricolae package [66] in R v3.5 (http://www.R-project.org). Mean

differences between treatments were compared using Tukey's test and a value $p < 0.05$ was regarded statistically significant. All graphs were generated using Sigma Plot Software (Version 14.5, Systat Software, Inc.).

3. Results and discussion

3.1. Characterization of LI-CuO nanoparticles

Multifunctional LI-CuO NPs were synthesized via an environmentally benign bio-reduction method using LILE and metallic salt ($CuSO_4{\cdot}5H_2O$). As the reduction proceeded, the color of the reaction mixture transformed from light blue to brownish-black attributed to the formation of LI-CuO NPs. The color change is caused by the interplay of phytochemicals in the LILE like phenols, saponin, and alkaloids that contributed to the synthesis of CuO NPs [4,6,37]. *L. indica* leaf extracts has been reported to have abundant active compounds [53,56–58]. Moreover, the optical properties of LI-CuO NPs synthesized was analyzed utilizing UV–vis absorption spectroscopy. The fabrication of CuO NPs was validated by observing a characteristic absorption peak in the UV–vis spectrum within the range of 200–800 nm. Specifically, a strong absorbance peak at 320 nm was recorded, indicating the formation of LI-CuO NPs (Fig. 1) and associated to the surface plasmon resonance (SPR) of copper oxide particles [67]. This strong peak signifies the repulsion of free electrons on the surface of NPs [67]. The occurrence of SPR absorption is indicative of the size and morphology of nanoparticles [6]. Additionally, the absorption peak at 320 nm corresponds to the inter-band transition of core electrons within the copper metal present in CuO NPs [43]. Several factors including crystallinity, crystallite size, shape, precursor concentration, and aggregations can influence the SPR peak of NPs [68]. In this study, the appearance of a single SPR peak implies that LI-CuO NPs are spherical [6,69] and the broader absorbance peak is the feature of the wide size distribution [21].

The functional groups surfacing biosynthesized LI-CuO NPs were examined by FTIR spectroscopy. Fig. 2 displays the spectra of fabricated LI-CuO NP, highlighting key vibrational bands at 998, 1498, 1737, 2227, 2982, 3501, and 3953 cm^{-1}. The major functional bands in the spectrum of LI-CuO NPs were noted at 2982 cm^{-1}, representing medium stretching vibration of aliphatic $–CH_2$ groups (alkane), whereas a strong peak at 2227 cm^{-1} and weak peak at 1735 cm^{-1} were found to be alkyne stretching (C≡C) and aldehyde (C═O) groups, respectively [70]. Hydroxyl groups (O–H), overlapping with NH stretching vibrations of amines, were detected between 3501 and 3953 cm^{-1} [71]. Furthermore, the strong peaks at 1364 cm^{-1} and 1498 cm^{-1} showed the presence of aliphatic aromatics (CH) and phenols [67]. With the slight shift in band compared to the LILE, LI-CuO NPs possessed bioactive phytochemicals dominantly present in the LILE indicating their role as reducing agents for Cu during biosynthesis as well as serving as capping materials [67,72].

The average LI-CuO NPs were analyzed using DLS to determine their average size, size distribution, polydispersity index (PDI) and surface charge. In aqueous solution, the average size and zeta potential of LI-CuO NPs were 93.5 nm and −20 mv, respectively (Fig. 3a and b). The higher negative zeta potential denoted the strong repulsion forces among particles, enhancing stability and quality [38,73]. Stability of nanoparticles is directly related to the magnitude of surface charge measured in terms of zeta potential [73]. In addition, the polydispersity index (PDI) of LI-CuO NPs was about 0.152 which signified a monodisperse distribution or homogeneity in colloidal solution. NPs with monodispersed size distribution and PDI value less than 1.0 have been regarded as having good colloidal stability [74].

The structural characterization of LI-CuO NPs was investigated using TEM and SEM coupled with EDX analyses. The SEM and TEM images revealed the spherical nanoparticles (Fig. 4a and b). Some aggregations in SEM images were observed compared to TEM analysis. The agglomeration of particles is likely due to the accumulation of different reducing agents from plant extract or their magnetic interactions [75,76]. SAED pattern revealed concentric rings, indicating the presence of numerous crystallites of agglomerated LI-CuO NPs (Fig. 4c), facilitating their excellent dispersion in bio-reduced aqueous solution, even on the macroscopic scale. The aggregation of Cu may result from the thermodynamic stability of CuO blocking oxidation than Cu ions [77]. The EDX analysis confirmed elemental composition, showing copper (39.85 %), oxygen (30.93 %), carbon (25.57.8 %), potassium (0.55 %) and sulfur (3.74 %) (Fig. 4 b & d). Absorption peaks near 1.0 and 8.0 keV in the EDX spectrum correspond to Cu atoms. In EDX spectrum, C and S

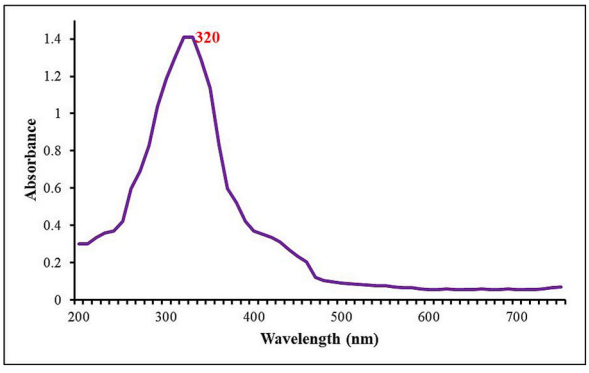

Fig. 1. UV–vis absorbance spectra of LI-CuO NPs in aqueous solution.

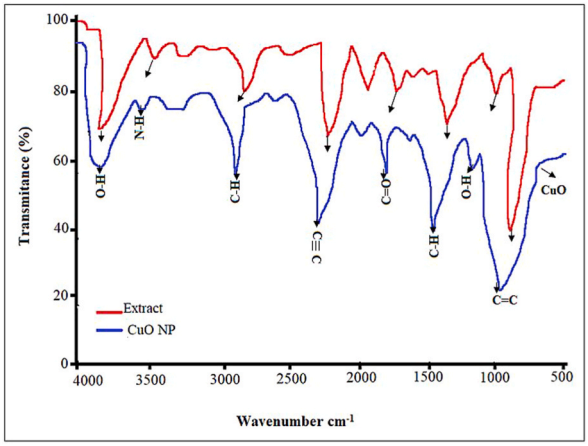

Fig. 2. Comparison of the FTIR spectra of the *L. indica* leaf extract and LI-CuO NPs. Each peak in the LI-CuO NPs indicates the functional group of the phytochemical involved in the reduction and stabilization leading to nanoparticle synthesis. Arrows pointing to the corresponding functional group.

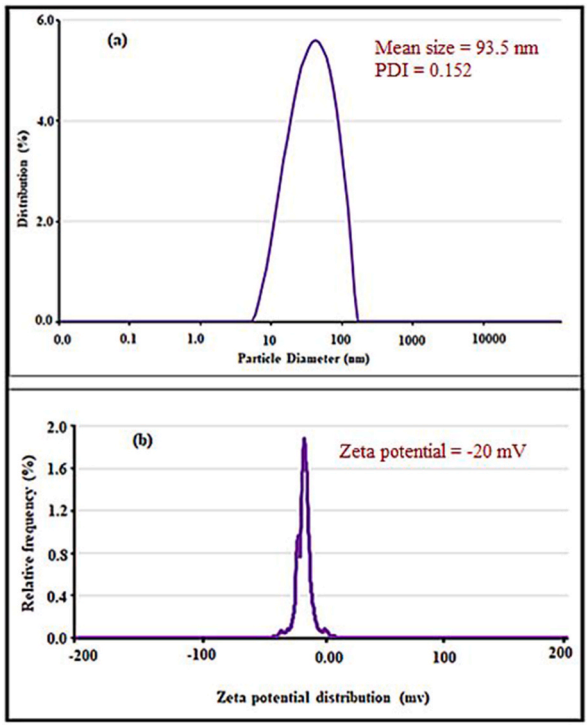

Fig. 3. Size distribution (a) and zeta potential (b) of LI-CuO NPs in aqueous suspension.

might be derived from phytochemicals (carbohydrates, flavonoids, phenols, saponins and tannins) from the leaf extract and $CuSO_4$ precursor [7,14].

XPS analysis results for the green-synthesized LI-CuO NPs is provided in Fig. 5. Occurrence of copper is confirmed by peaks of relative intensity Cu2p1, Cu2p3, Cu LMM and Cu 3p. Additionally, peaks corresponding to biomolecule-related elements such as O (1s and KL1), carbon (C1s and CKLL), and S (S2p and S2s) were observed, with C1s indicating the presence of carbon-containing functional groups [78]. The O1s major peak at 531.2 eV for O═C, O (Cu (II), C, H) [78] indicated the presence of Cu as +2 oxide in the synthesized LI-CuO NPs [71]. XRD analysis, shown in Fig. 6 revealed major Bragg's diffraction peaks at 32.51°, 35.53°, 38.75°, 46.31°, 48.76°, 53.58°, 58.31°, 61.58°, 66.24° and 68.08° corresponding to crystallographic planes of (110), (−111), (111), (−112), (−202), (020), (202), (−113), (−311) and (220), respectively. The sharpness of the peaks indicated that the synthesized LI-CuO NPs are monoclinic and crystalline nature [79] with JCPDS-80-0076. Using the Scherrer formula, the average crystal size was estimated to be

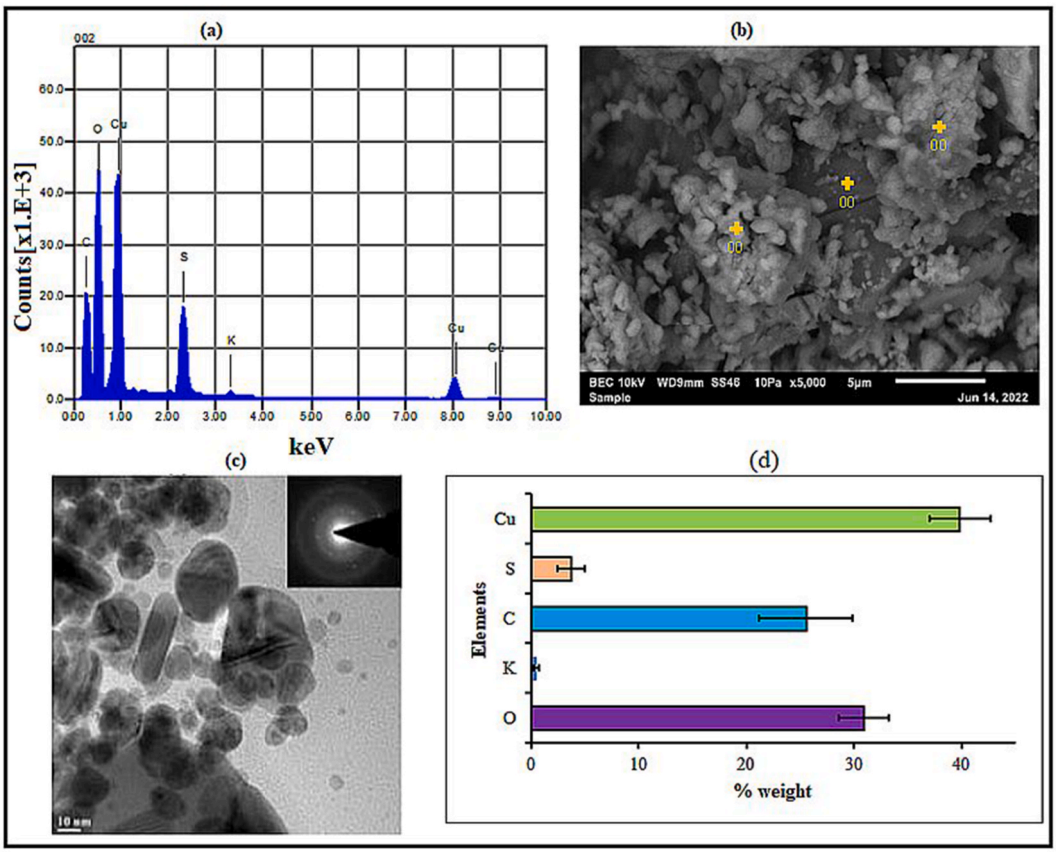

Fig. 4. EDX spectra (a), SEM micrographs (b) TEM image (c) and weight element composition (d) of biosynthesized LI-CuO NPs. Inset in TEM image is SAED pattern of the particles.

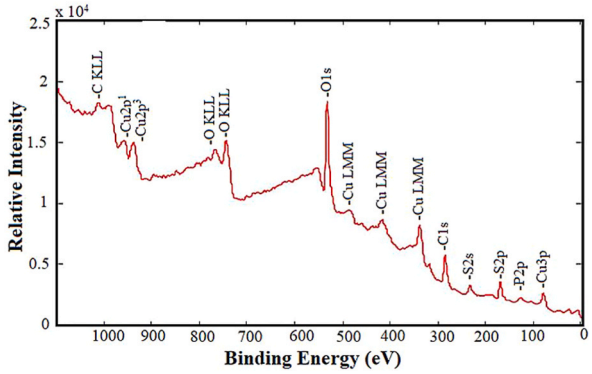

Fig. 5. XPS spectra of the synthesized LI-CuO NPs.

36 nm from the XRD spectrum's peak width.

3.2. Antimicrobial activity of LI-CuO nanoparticles

Globally, the rise in antibiotic resistance and the prevalence of hospital-acquired infections have exacerbated the incidence and epidemics of pathogenic microbes [3,4]. To avert these issues there is great importance in biomedical applications of biosynthesized nanoparticles including CuO NPs. In the present study, we evaluated the antimicrobial potential efficacy of LI-CuO NPs against pathogenic Gram-negative (*E. coli* and *S. typhimurium*), and Gram-positive (*S. aureus* and *L. monocytogenes*) bacteria employing the agar well diffusion method. LI-CuO NPs demonstrated stronger antimicrobial activity than LILE in a concentration-dependent pattern

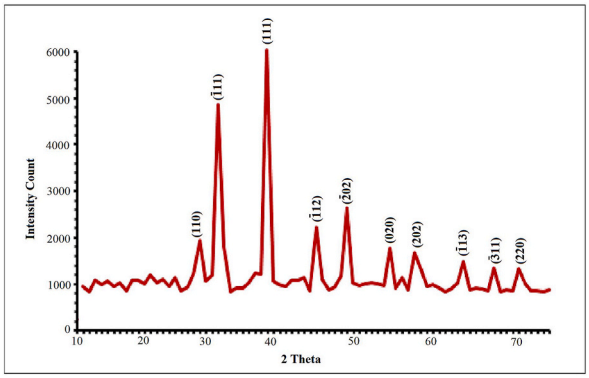

Fig. 6. XRD pattern of the synthesized LI-CuO NPs along with JCPDS Data.

(Fig. 7, Table 1). Indeed, this aligns with other studies that reported the antibacterial activity of CuO NPs and other metallic oxide nanoparticles [16–20] increases with a rise in concentration [80]. However, the antimicrobial effect of nanoparticles relies on different factors including morphology, solubility and surface functional groups [67]. The antibacterial activity of LI-CuO NPs revealed greater susceptibility of Gram-negative bacteria, *E. coli* and *S. typhimurium*, with larger zone of inhibition (ZOI) diameters of 17.1 mm and 16.4 mm, respectively, compared to Gram-positive bacteria *L. monocytogenes* and *S. aureus* with ZOI of 12.2 mm and 14.7 mm, respectively at 100 μg L^{-1} (Fig. 7, Table 1). The MIC and MBC values also showed higher susceptibility of Gram-negative bacteria over Gram-positive bacteria than (Fig. 8). This discrepancy in sensitivity could stem from the unique and single peptidoglycan layer of

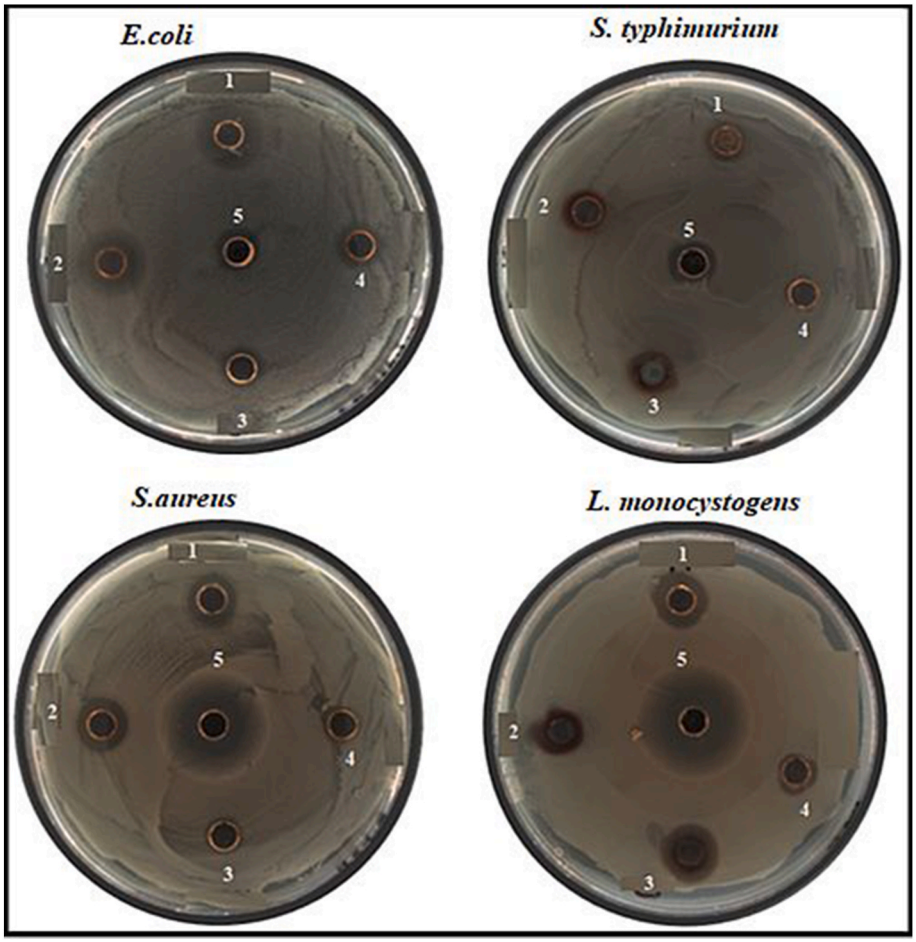

Fig. 7. Agar well diffusion method for antimicrobial activity as zones of inhibition observed three LI-CuO NPs concentrations including 1(200 μg/mL), 2 (100 μg/mL), 3 (50 μg/mL), 4 (LILE) and 5 (streptomycin) against gram-positive and gram-negative bacteria.

Table 1
Zone of inhibition (mm) of streptomycin, LILE and LI-CuO NPs against gram-negative and gram-positive foodborne pathogens. Values are given as Mean ± SD.

Bacteria	Streptomycin	LILE	LI-CuO NPs (μg/mL)		
	100	100	100	75	50
E. coli	10.5 ± 0.5	10.1 ± 0.3	17.1 ± 0.8	16.4 ± 0.4	11.3 ± 0.3
S. typhimurium	21.2 ± 1.4	11.3 ± 0.5	16.4 ± 0.2	11.21 ± 0.6	11.4 ± 0.5
S. aureus	20.5 ± 1.2	8.1 ± 0.7	14.7 ± 0.6	13.4 ± 0.9	8.2 ± 0.1
L. monocytogenes	11.3 ± 0.4	6.8 ± 0.2	12.2 ± 0.7	11.5 ± 0.5	9.3 ± 0.3

Gram-negative bacteria, contrasting with the thick peptidoglycan layer in Gram-positive bacteria [81]. While the highest MIC value of 46.4 μg $mL^{-1}$was recorded for the Gram-positive bacterium, *S. aureus* the lowest MIC value of 32.4 μg mL^{-1} was noted for the Gram-negative bacterium, *E. coli*. The highest MBC recorded for LI-CuO NPs was 95.6 μg mL^{-1} for *S. aureus* while the lowest MBC value of 62.5 μg mL^{-1} was observed for *E. coli*. Consistently, in a study by Andualem et al. [82], it was found that CuO NPs exhibited greater efficacy against Gram-negative bacterial strains. Electrostatic interactions between CuO NPs and bacterial cell walls, particularly Gram-negative bacteria like *E. coli* might significantly contributed to their antimicrobial efficacy compared to Gram-positive bacteria [83]. The bactericidal potential of LI-CuO NPs could also be explained by the bioactive molecules capping the NPs as highlighted in the FTIR analysis and their small size indicated in DLS analysis [21]. Moreover, the strong antibacterial activity of biosynthesized LI-CuO NPs may be linked to surface charge/zeta potential, which determines electrostatic interactions, adsorption and subsequent penetration of bacterial cells by the nanoparticles [84].

Copper oxide nanoparticles exhibit diverse antimicrobial mechanisms, disrupting RNA and DNA replication, ATP production, and stimulating oxidative stress through generating reactive free radicals and modulating signal transduction pathways, ultimately leading to bacterial cell membrane damage, lysis and death [67,85,86]. Furthermore, NPs can efficiently enter the cell through porins on the bacterial plasma membrane and possibly result in ionic imbalance and protein and enzyme leakage that eventually alters cell growth [6,7,21]. Studies have also suggested that CuO NPs' release of Cu^{2+} ions in the media affects bacterial respiration and other important biochemical processes [85]. The Cu^{2+} ions released can bind to thiol groups in key bacterial enzymes and proteins, leading to their inactivation and bacterial death [85]. Additionally, the accumulation of Cu^{2+} ions can outcompete essential ions in the cells such as Fe^{2+}, impeding proper cofactor binding to proteins and resulting in protein dysfunction [87,88].

3.3. Antioxidant activity of LI-CuO nanoparticles

Cellular oxidation, leading to the generation of free radicals and reactive oxygen species (ROS), is implicated in various human disorders by damaging antioxidant systems and causing cell death [89]. However, antioxidant activity involves mechanisms such as hydrogen abstraction, termination of free radical-driven chain reactions, peroxide removal, metal ion chelation, and radical scavenging [90]. Factors contributing to antioxidant activity include the absorption, neutralization of free radicals, and quenching of singlet and triplet oxygen [91]. In this study, we assessed the in vitro radical scavenging potential of LI-CuO NPs using the DPPH assay, comparing their activity with LILE and ascorbic acid, a standard antioxidant, as shown in Fig. 9. LI-CuO NPs exhibited significant variation in concentration-dependent radical scavenging activity ($P < 0.05$). The DPPH radical scavenging activities ranged from 7.25 to 85.41 %, 25.26–93.3 % and 10.2–97.6 % for LILE, ascorbic acid and LI-CuO NPs, respectively. Notably, at 400 μg mL^{-1}, LI-CuO NPs displayed a scavenging activity of 97.6 %, surpassing that of the standard (93.3 %). In support of the FTIR analysis, the highest antioxidant properties of LI-CuO NPs might be associated with the presence of phytochemical functional groups from LILE acting as capping agents [85]. In addition, nuclear magnetic resonance characterization showed that LILE contains notable phytochemicals such as gallic acid, isovitexin, luteolin, vitexin, orientin, astragalin, catechin, rutin and quercetin with antioxidant properties [53,56–58].

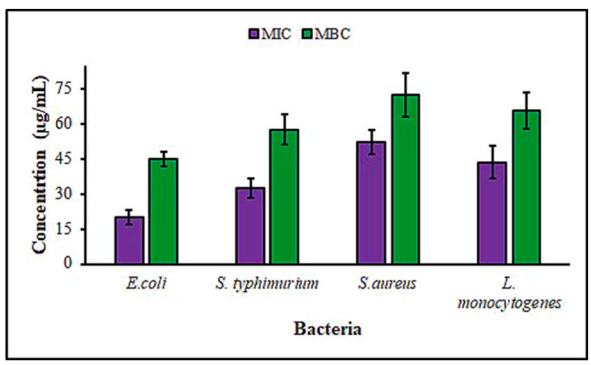

Fig. 8. Minimum inhibitory/bactericidal concentrations (MIC/MBC) of LI-CuO NPs against four foodborne pathogens. Values are presented as mean ± SD.

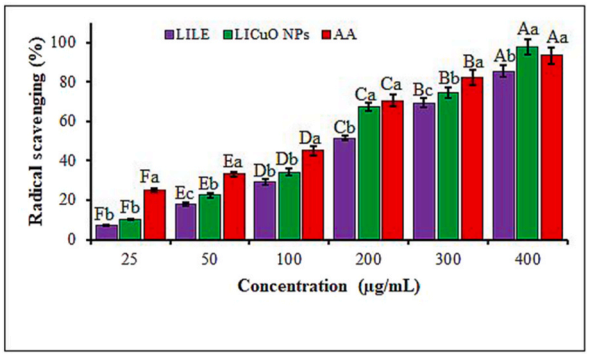

Fig. 9. The antioxidant activity of LILE and LI-CuO NPs measured using DPPH radical scavenging assay. AA represents ascorbic acid. Different lower-case letters denote significant differences ($p \leq 0.05$) among AA, LILE and LI-CuO NPs at a particular concentration, whereas uppercase letters denote significant differences across different concentrations for a particular antioxidant.

Additionally, antioxidants such as phenols and flavonoids, due to their redox properties, play a crucial role in absorbing, neutralizing free radicals, and quenching singlet and triplet oxygen [83,92,93].

3.4. Effect of LI-CuO nanoparticles on seed germination

Critical plant development stages, including seed germination and early seedling establishment are impacted by diverse biotic and abiotic factors [94,95]. Herein, to evaluate the phytotoxicity of biosynthesized LI-CuO NPs, we conducted seed germination tests as a direct and reliable method [96]. Results showed that LI-CuO NPs revealed an enhanced seed germination at lower concentrations (up to 100 mg L^{-1}) but inhibited it at higher concentrations (Fig. 10). Specifically, at the highest concentration (200 mg L^{-1}), only 12 % of seeds germinated. Maximum percent germination (96.52 %) was observed at 100 mg L^{-1}, comparable to the control (94.28 %). This inhibition at high concentrations underscores the potential toxicity of CuO NPs on mustard seeds [97]. Our findings align with existing studies on various plant species, demonstrating a pattern where seed germination is enhanced at lower concentrations of CuO NPs but significantly inhibited at higher concentrations [98–100]. Notably, CuO NPs have been reported to completely inhibit germination in species such as *Cucumis sativus* [101], *Lactuca sativa* [102], and *Vigna radiata* [37,103]. Conversely, in some instances, the germination of lettuce and carrot seeds remained unaffected by CuO NPs [104]. This variability suggests species-specific responses to CuO NPs, influenced by nanoparticles property, nature of the reducing and stabilizing agents used and synthesis methods [37,100]. However, the mechanistic effects of LI-CuO NPs on mustard germination at low concentrations require further investigation.

3.5. Photocatalytic effect of LI-CuO NPs dye degradation and reusability

The photocatalytic activity of the biofabricated LI-CuO NPs was evaluated for the degrading methylene blue (MB), a common dye

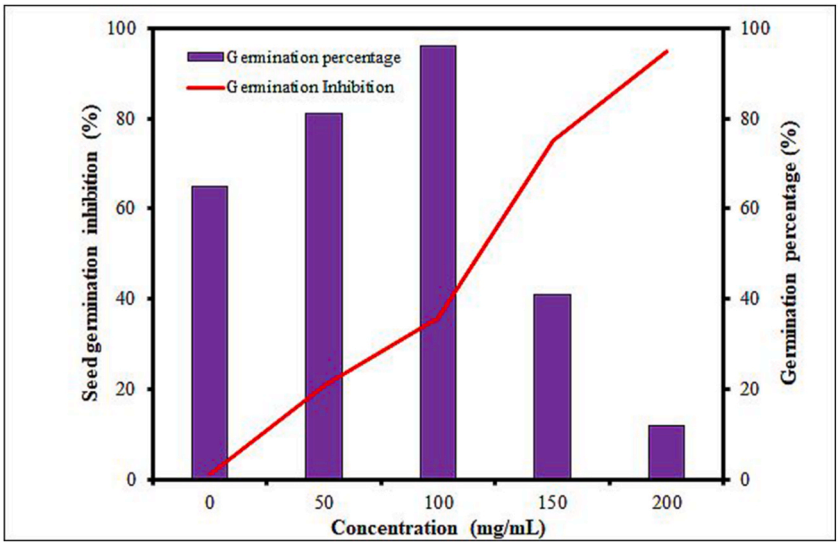

Fig. 10. Effect LI-CuO NPs on mustard (*Brassica juncea*) seed germination characteristics.

used in textile and medicine that causes various environmental concerns [105] under sunlight irradiation. A distinctive UV–vis absorption spectrum of MB solution degradation at 150 μg/mL across time is provided in Fig. 11a. The peak absorption bands were recorded between 400 and 800 nm at 0, 30, 60, 90, 120 and 150 min. The prominent peak was recorded at 664 nm, indicating the presence of MB dye. However, as time progressed, the intensity of this band became broad and weak, suggesting complete degradation of MB into its protonated form [105]. Complete degradation was achieved within 150 min using the highest LI-CuO NPs concentration (150 μg/mL) (Fig. 11 a-c) with a remarkable degradation efficiency of 97.6 %. In addition, MB degradation increased proportionally with the LI-CuO NPs concentration gradient (Fig. 11b). Specifically, degradation efficiencies of 19.31, 32.2, 51.3, 61.5, 79.7 and 97.6 % were achieved when treated with 5, 10, 25, 50, 100 and 150 μg/mL of LI-CuO NPs, respectively.

Several efforts have been made to unravel the mechanism behind the photodegradation of MB dye catalyzed by CuO NPs under sunlight irradiation [106–108]. Thammavongsy et al. [109] highlighted the role of metallic nanoparticles in modulating the redox potential, resulting the photocatalytic degradation of MB. Biosynthesized CuO NPs have been reported as effective redox catalysts owing to their electron transmission phenomenon [108]. The degradation of free or adsorbed MB molecules onto the LI-CuO NPs surface could be occurred through hydroxyl radicals that are formed from the reaction between the positive hole in the NPs and H_2O [108]. Also, Sharma and Dutta [110] showed that hydroxyl radicals formed to take part in the degradation when applying CuO NPs as catalysts. Overall, compared to CuO NPs synthesized using other plant extracts [111–120], the biosynthesized LI-CuO NPs exhibited superior performance in degrading MB dye (Table 2). However, it's noteworthy that the photocatalytic activity of metallic nanoparticles is influenced by different factors including reaction time, concentration, morphology, shape and size of the particles [77,121,122]. In this study, the biosynthesized LI-CuO NPs demonstrated remarkably small particle sizes, align with their high photocatalytic efficiency. Moreover, the presence of phenol and flavonoid groups in the extract used for biosynthesis promoted electron transfer to the conduction band of CuO, enhancing the generation of superoxide radicals and thereby accelerating the photodegradation process catalyzed by LI-CuO NPs [108].

Reusability test of the synthesized CuO NPs for photocatalytic treatment across different cycles is a crucial step for large-scale applications [88,123]. In the present study, the reusability of LI-CuO NPs was assessed under maximum concentration (150 μg/mL), where optimal catalytic activity was observed for 150 min. Initially, the activity of LI-CuO NPs in degrading MB was found to be 97.6 ± 0.9 %. However, over successive cycles, there was a gradual decrease to 95.2 ± 3.6 %, 91.7 ± 02.3 %, 88.4 ± 2.2 %, 86.5 ± 3.1 % and 83.2 ± 2.5 % after five cycles (Fig. 12). These reusability test results suggested the remarkable stability and robustness of LI-CuO NPs for MB degradation and elimination. This finding is consistent with previous studies that have investigated the catalytic activity and reusability of CuO NPs in MB degradation under light conditions [71,124]. These studies underscore the practical value of CuO NPs, emphasizing their robustness and suitability for repeated use in MB elimination processes.

3.6. Potential of LI-CuO nanoparticles in wastewater treatment

While the global demand for clean freshwater continues to rise, the pervasive issue of water pollution remains a significant impediment to its availability [125]. Addressing the challenges associated with treating industrial and agricultural wastewater, particularly in regions facing water scarcity, has become a paramount concern. Recycling and water conservation have been identified as potential solutions to mitigate this challenge, with wastewater treatment rendering a key role in curbing the toxic impact of pathogens and pollutants. Furthermore, incorporating active substances with antimicrobial properties can enhance the quality of treated wastewater. In this study, efficiency of different concentrations of LI-CuO NPs (10, 25, 50, 100 and 150 mg L^{-1}) in wastewater treatment was assessed. Coagulation with the application of LI-CuO NPs yielded a significant increase in turbidity removal with rising concentration ($p < 0.05$, Fig. 13). The efficiency of turbidity removal ranged from 23.2 % to 95.6 % across LI-CuO NPs concentrations of 10–150 mg L^{-1}. Notably, the lowest turbidity recorded was 7 NTU at 150 mg L^{-1}, meeting World Health Organization's standards for drinking water. The application of plant seeds and leaves as natural coagulants has been well-studied [126–128]. Active coagulants present in plants, such as proteins and phytochemicals, are soluble and can be extracted using water [126,128] and have been reported to enhance turbidity removal [129,130]. FTIR analysis of LI-CuO NPs revealed various functional groups including carboxylic acid (C═O), hydroxyl (–OH), and aliphatic amines (N–H), suggesting the presence of positively and negatively charged species. This observation implies that these functional groups could enhance coagulation-flocculation by neutralizing pollutants in the wastewater [131]. However, for large-scale wastewater treatment and reusability, a more in-depth analysis of conditions affecting coagulation and the underlying mechanisms requires further investigation.

4. Conclusions

Employing an eco-friendly approach, we successfully synthesized multifunctional LI-CuO NPs utilizing an extract derived from *L. indica* leaves as both reducing and capping agent. The resulting nanoparticles demonstrated monodispersed, a spherical shape, crystalline structure, and high stability. Our investigation revealed that LI-CuO NPs exhibited significant inhibitory effects on a spectrum of pathogens, including *E. coli*, *S. typhimurium*, *S. aureus*, and *L. monocytogenes*. Additionally, these biofabricated nanoparticles displayed noteworthy antioxidant activity and enhanced seed germination at lower concentrations. LI-CuO NPs exhibited excellent photocatalytic performance, with a degradation efficiency of 97.6 % and remarkable reusability. Furthermore, these nanoparticles showed promise in wastewater treatment by effectively reducing turbidity through coagulation. In conclusion, the biosynthesized LI-CuO NPs demonstrated a diverse range of properties, including antimicrobial, antioxidant, photocatalytic, and coagulation. These findings highlight the potential applications of LI-CuO NPs including seed priming, environmental remediation, and biomedical research. Despite these promising outcomes, further research is essential to fully unlock the potential of LI-CuO NPs

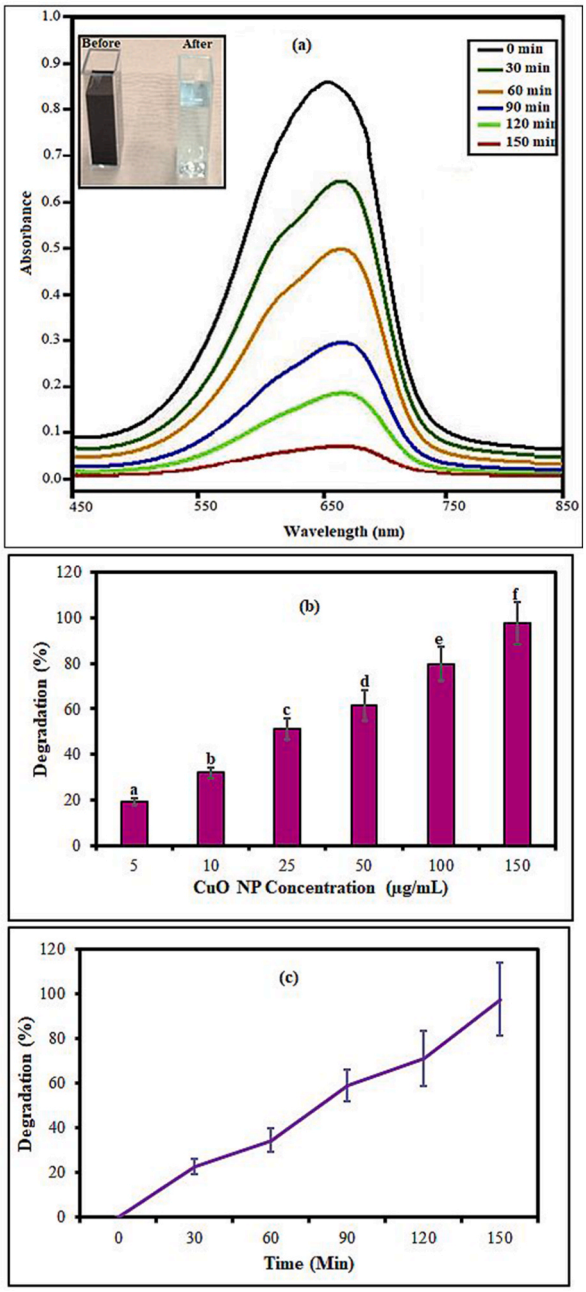

Fig. 11. Photocatalytic degradation of methylene blue using LI-CuO NPs; (a) absorbance of methylene blue treated with 150 µg/mL LI-CuO NPs across different times; (b) degradation efficiency of different concentrations of LI-CuO NPs; (c)efficiency of degradation of methylene blue across time at 150 µg/mL LI-CuO NPs. (For interpretation of the references to color in this figure legend, the reader is referred to the Web version of this article.)

and optimize their properties tailored for specific applications.

Funding

This research was supported by the United States Department of Agriculture National Institute of Food and Agriculture (USDA-NIFA) Evans-Allen Grant scheme 180835-82601.

Table 2
Comparison of photocatalytic activity of CuO-NPs prepared from different plant extracts.

Synthesis Method	Time (min)	Light Source	Degradation (%)	Ref
L. indica	150	Sunlight	97.6	Present study
Psidium guajava	12	Visible light	91	[112]
Ocimum americanum	200	Sunlight	71.06	[113]
Ferulago angulata	150	Sunlight	93	[114]
Verbascum thapsus	120	Sunlight	99.3	[115]
Bergenia ciliata	135	Sunlight	92.3	[116]
Cymbopogon citratus	300	Sunlight	80	[117]
Gloriosa superba	100	Sunlight	93	[118]
Solanum lycopersicum	300	Sunlight	97	[119]
Madhuca longifolia	120	Sunlight	77	[120]

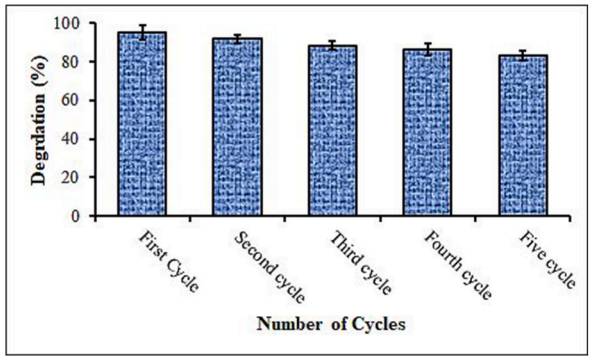

Fig. 12. Reusability of green-synthesized LI-CuO NPs for degradation of MB for several cycles. (For interpretation of the references to color in this figure legend, the reader is referred to the Web version of this article.)

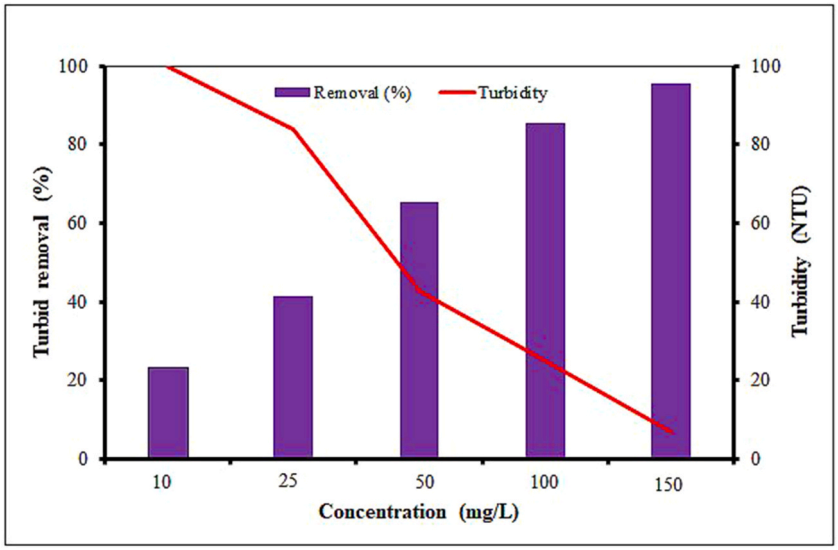

Fig. 13. Turbid removal efficiency of LI-CuO NPs against wastewater.

Data availability statement

Most of the data are available in all Tables and Figures of the manuscript. Additionally, the data will be available by the corresponding author on request without undue reservation.

CRediT authorship contribution statement

Addisie Geremew: Writing – original draft, Project administration, Methodology, Data curation, Conceptualization. **Lenaye Palmer:** Investigation. **Andre Johnson:** Investigation. **Sheena Reeves:** Writing – review & editing, Methodology, Investigation. **Nigel Brooks:** Jr, Methodology, Investigation. **Laura Carson:** Writing – review & editing, Supervision, Software, Resources, Project administration, Methodology, Conceptualization.

Declaration of competing interest

The authors declare that they have no known competing financial interests or personal relationships that could have appeared to influence the work reported in this paper.

Acknowledgments

The authors gratefully acknowledge the Cooperative Agricultural Research Center in the College of Agriculture and Human Sciences at Prairie View A&M University, United States, for generously providing the research facilities necessary for conducting the entirety of this scientific investigation. Additionally, the authors extend their appreciation to the Surface Characterization Facility within the Department of Chemistry and Physics for their invaluable support.

References

[1] N.P. Webb, N.A. Marshall, L.C. Stringer, M.S. Reed, A. Chappell, J.E. Herrick, Land degradation and climate change: building climate resilience in agriculture, Front. Ecol. Environ. 15 (8) (2017) 450–459.
[2] P. Shukla, P. Chaurasia, K. Younis, O.S. Qadri, S.A. Faridi, G. Srivastava, Nanotechnology in sustainable agriculture: studies from seed priming to post-harvest management, Nanotechnol. Environ. Eng. 4 (2019) 11.
[3] R. Jiang, W. Ahmed, H. Daud, D. Ahmed, S. Al-Rejaie, M. Awais, I. Muhammad, M.I. Khan, M.M. Jalal, O.M. Alshehri, H. Mahnashi, Prevalence of drug-resistant microbes in sepsis cases of catheter and fistula-based hemodialysis, Saudi J. Biol. Sci. 28 (2021) 7443–7449.
[4] A.A. Badawy, N.A.H. Abdelfattah, S.S. Salem, M.F. Awad, A. Fouda, Efficacy assessment of biosynthesized copper oxide nanoparticles (CuO-NPs) on stored grain insects and their impacts on morphological and physiological traits of wheat (*Triticum aestivum* L.), Plant, Biology 10 (2021) 233.
[5] X.P. Wang, Q.Q. Li, Z.M. Pei, S.C. Wang, Effects of zinc oxide nanoparticles on the growth, photosynthetic traits, and antioxidative enzymes in tomato plants, Biol. Plant. (Prague) (2018) 62, https://doi.org/10.1007/s10535-018-0813-4.
[6] A. Geremew, L. Carson, S. Woldesenbet, Biosynthesis of silver nanoparticles using extract of *Rumex nepalensis* for bactericidal effect against food-borne pathogens and antioxidant activity, Front. Mol. Biosci. 9 (2022) 991669.
[7] G. Sharmila, R.S. Pradeep, K. Sandiya, S. Santhiya, C. Muthukumaran, J. Jeyanthi, N.M. Kumar, M. Thirumarimurugan, Biogenic synthesis of CuO nanoparticles using *Bauhinia tomentosa* leaves extract: characterization and its antibacterial application, J. Mol. Struct. 165 (2018) 288e292.
[8] V. Bharat, S. Shubham, D. Jagdish, P. Amol, K. Renuka, Smart water management system in cities, ICBDAC (2017) 267–271, https://doi.org/10.1109/ICBDACI.2017.8070846.
[9] M.R. Kiani, M.R. Rahimpour, Aquatic/water environment contamination, treatment, and use, in: A. Figoli, Y. Li, A. Basile (Eds.), Current Trends and Future Developments on (Bio-) Membranes, Elsevier, 2020, pp. 213–238.
[10] K. Selvam, G. Albasher, O. Alamri, C. Sudhakar, T. Selvankumar, V. Vijayalakshmi, L. Vennila, Enhanced photocatalytic activity of novel *Canthium coromandelicum* leaves based copper oxide nanoparticles for the degradation of textile dyes, Environ. Res. 211 (2022) 113046.
[11] N.R. Dhineshbabu, V. Rajendran, N. Nithyavathy, R. Vetumperumal, Study of structural and optical properties of cupric oxide nanoparticles, Appl. Nanosci. 6 (2016) 933–939.
[12] M. Grigore, E. Biscu, A. Holban, M. Gestal, A. Grumezescu, Methods of synthesis, properties and biomedical applications of CuO nanoparticles, Pharmaceuticals 9 (2016) 75.
[13] R. Sivaraj, P.K.S.M. Rahman, P. Rajiv, S. Narendhran, R. Venkatesh, Biosynthesis and characterization of *Acalypha indica* mediated copper oxide nanoparticles and evaluation of its antimicrobial and anticancer activity, Spectrochimica Acta -A: Mol. Biomol Spectrosc 129 (2014) 255–258.
[14] D. Renuga, J. Jeyasundari, A.S.S. Athithan, Y.B.A. Jacob, Synthesis and characterization of copper oxide nanoparticles using *Brassica oleracea* var. itatic extract for its antifungal application, Mater. Res. Express 7 (2020) 4500.
[15] F. Samari, L. Baluchi, H. Salehipoor, S. Yousefinejad, Controllable phyto-synthesis of cupric oxide nanoparticles by aqueous extract of *Capparis spinosa* (caper) leaves and application in iron sensing, Microchem. J. 150 (2019) 1041582.
[16] A. Muthuvel, M. Jothibas, C. Manoharan, Effect of chemically synthesis compared to biosynthesized ZnO-NPs using *Solanum nigrum* leaf extract and their photocatalytic, antibacterial and in-vitro antioxidant activity, J. Environ. Chem. Eng. 8 (2020) 103705, https://doi.org/10.1016/j.jece.2020.103705.
[17] M.A. Tahereh, M.K. Negar, S.S. Abbas, *In situ* production and deposition of nanosized zinc oxide on cotton fabric, Iran. J. Chem. Chem. Eng. 40 (2021) 1–9.
[18] M.K. Negar, M. Yaqoubi, Green synthesis and characterization of bismuth oxide nanoparticle using *Mentha pulegium* extract, Iran. J. Pharm. Res. (IJPR) 19 (2) (2020) 70–79, https://doi.org/10.22037/ijpr.2019.15578.13190.
[19] S. Hajiashrafi, N. Motakef-Kazemi, Green synthesis of zinc oxide nanoparticles using parsley extract, Nano Res. J 3 (1) (2018) 44–50, https://doi.org/10.22034/nmrj.2018.01.007.
[20] A. Geremew, L. Carson, S. Woldesenbet, H. Wang, S. Reeves, N. Jr. Brooks, P. Saganti, A. Weerasooriya, E. Peace, Effect of zinc oxide nanoparticles synthesized from *Carya illinoinensis* leaf extract on growth and antioxidant properties of mustard (*Brassica juncea*), Front. Plant Sci. 14 (2023) 1108186, https://doi.org/10.3389/fpls.2023.1108186.
[21] M. Fernández-Arias, M. Boutinguiza, J. del Val, A. Riveiro, D. Rodríguez, Arias-González, J. Gil, J. Pou, Fabrication and deposition of copper and copper oxide nanoparticles by laser ablation in open air, Nanomaterials 10 (2020) 300.
[22] F. Duman, I. Ocsoy, F.O. Kup, Chamomile flower extract directed CuO nanoparticle formation for its antioxidant and DNA cleavage properties, Mater. Sci. Eng. C 60 (2016) 333–338.
[23] D. Rehana, D. Mahendiran, R.S. Kumar, A.K. Rahiman, Evaluation of antioxidant and anticancer activity of copper oxide nanoparticles synthesized using medicinally important plant extracts, Biomed. Pharmacother. 89 (2017) 1067–1077.
[24] C.M. Park, K.H. Chu, J. Heo, N. Her, M. Jang, A. Son, Y. Yoon, Environmental behavior of engineered nanomaterials in porous media: a review, J. Hazard Mater. 309 (2016) 133–150.
[25] E.F.B. Zeid, I.A. Ibrahem, W.A.A. Mohamed, A.M. Ali, Study the influence of silver and cobalt on the photocatalytic activity of copper oxide nanoparticles for the degradation of methyl orange and real wastewater dyes, Mater. Res. Express 7 (2020) 026201.
[26] M. Dinesh, S.M. Roopan, C.I. Selvaraj, P. Arunachalam, *Phyllanthus emblica* seed extract mediated synthesis of Pd NPs against antibacterial, hemolytic and cytotoxic studies, J. Photochem. Photobiol. B Biol. 167 (2017) 64–71.

[27] S. Sagadevan, K. Pal, Z.Z. Chowdhury, Fabrication of CuO nanoparticles for structural, optical and dielectric analysis using chemical precipitation method, J. Mater. Sci. Mater. Electron. 28 (2017) 12591–12597.

[28] N. Zayyoun, L. Bahmad, L. Laanab, B. Jaber, The effect of pH on the synthesis of stable Cu2O/CuO nanoparticles by sol–gel method in a glycolic medium, Appl Phys A Mater Sc Process 122 (2016) 1–6.

[29] F. Mojtabazade, B. Mirtamizdoust, A. Morsali, P. Talemi, Sonochemical synthesis and structural determination of novel the nano-card house Cu (II) metal-organic coordination system, Ultrason. Sonochem. 35 (2017) 226e232.

[30] A. Bhattacharjee, M. Ahmaruzzaman, Microwave-assisted facile and green route for synthesis of CuO nanoleaves and their efficacy as a catalyst for reduction and degradation of hazardous organic compounds, J. Photochem. Photobiol. Chem. 353 (2018) 215–228.

[31] C.L. Carnes, J. Stipp, K.J. Klabunde, J. Bonevich, Synthesis, characterization, and adsorption studies of nanocrystalline copper oxide and nickel oxide, Langmuir 18 (2002) 1352–1359.

[32] R. Rahmatolahzadeh, M. Aliabadi, K. Motevalli, Cu and CuO nanostructures: facile hydrothermal synthesis, characterization and photocatalytic activity using new starting reagents, J. Mater. Sci. Mater. Electron. 28 (2017) 148e156.

[33] D. Han, H. Yang, C. Zhu, F. Wang, Controlled synthesis of CuO nanoparticles using TritonX-100-based water-in-oil reverse micelles, Powder Technol. 185 (2008) 286–290.

[34] W. Wang, Y. Zhan, X. Wang, Y. Liu, C. Zheng, G. Wang, Synthesis and characterization of CuO nanowhiskers by a novel one-step, solid-state reaction in the presence of a nonionic surfactant, Mater. Res. Bull. 37 (2002) 1093–1100.

[35] C.Y. Chiang, K. Aroh, S.H. Ehrman, Copper oxide nanoparticle made by flame spray pyrolysis for photoelectrochemical water splitting e Part I. CuO nanoparticle preparation, Int. J. Hydrogen Energy 37 (2012) 4871–4879.

[36] R. Katwal, H. Kaur, G. Sharma, M. Naushad, D. Pathania, Electrochemical synthesized copper oxide nanoparticles for enhanced photocatalytic and antimicrobial activity, J. Ind. Eng. Chem. 31 (2015) 173–184.

[37] J. Sarkar, N. Chakraborty, A. Chatterjee, A. Bhattacharjee, D. Dasgupta, K. Acharya, Green synthesized copper oxide nanoparticles ameliorate defence and antioxidant enzymes in *Lens culinaris*, Nanomaterials 10 (2020) 312.

[38] S.C. Mali, S. Raj, R. Trivedi, Biosynthesis of copper oxide nanoparticles using *Enicostemma axillare* (Lam.) leaf extract, Biochem. Biophys. Rep. 20 (2019) 100699.

[39] K.R. Reddy, Green synthesis, morphological and optical studies of CuO nanoparticles, J. Mol. Struct. 1150 (2017) 553–557.

[40] A. Dey, S. Manna, S. Chattopadhyay, D. Mondal, D. Chattopadhyay, A. Raj, S. Das, B.G. Bag, S. Roy, *Azadirachta indica* leaves mediated green synthesized copper oxide nanoparticles induce apoptosis through activation of TNF-a and caspases signaling pathway against cancer cells, J. Saudi Chem. Soc. 23 (2019) 222–238.

[41] G. Jayakumarai, C. Gokulpriya, R. Sudhapriya, G. Sharmila, C. Muthukumaran, Phytofabrication and characterization of monodisperse copper oxide nanoparticles using *Albizia lebbeck* leaf extract, Appl. Nanosci. 5 (2015) 1017–1022.

[42] K. Gebremedhn, M.H. Kahsay, M. Aklilu, Green synthesis of CuO nanoparticles using leaf extract of *Catha edulis* and its antibacterial activity, J. Pharm. Pharmacol. 7 (2019) 327–342.

[43] K. Singh, J. Singh, M. Rawat, Green synthesis of zinc oxide nanoparticles using *Punica granatum* leaf extract and its application towards photocatalytic degradation of Coomassie brilliant blue R-250 dye, SN Appl. Sci. 1 (2019) 624.

[44] P. Narasaiah, B.K. Mandal, N.C. Sarada, Biosynthesis of copper oxide nanoparticles from *Drypetes sepiaria* Leaf extract and their catalytic activity to dye degradation, IOP Conf. Ser. Mater. Sci. Eng. 263 (2017) 022012.

[45] P. Yugandhar, T. Vasavi, B. Shanmugam, P.U.M. Devi, K.S. Reddy, N. Savithramma, Biofabrication, characterization and evaluation of photocatalytic dye degradation efficiency of *Syzygium alternifolium* leaf extract mediated copper oxide nanoparticles, Mater. Res. Express 6 (2019) 065034.

[46] M. Hafeezl, R. Arshad, J. Khan, B. Akram, *Populus ciliata* mediated synthesis of copper oxide nanoparticles for potential biological applications, Mater. Res. Express 6 (2019) 055043.

[47] N. Sebeia, M. Jabli, A. Ghith, Biological synthesis of copper nanoparticles, using *Nerium oleander* leaves extract characterization and study of their interaction with organic dyes, Inorg. Chem. Commun. 105 (2019).

[48] A.A. Yaqoob, T. Parveen, K. Umar, M.N. Rahim, Role of nanomaterials in the treatment of wastewater: a review, Water 12 (2020) 495.

[49] W. Xie, Q. Gao, D. Wang, W. Wang, J. Yuan, Z. Guo, H. Yan, X. Wang, X. Sun, L. Zhao, Melatonin potentiates "inside-out" nano-thermotherapy in human breast cancer cells: a potential cancer target multimodality treatment based on melatonin-loaded nanocomposite particles, Int. J. Nanomed. 12 (2017) 7351–7363.

[50] J. Lin, X. Weng, X. Jin, M. Megharaj, R. Naidu, Z. Chen, Reactivity of iron-based nanoparticles by green synthesis under various atmospheres and their removal mechanism of methylene blue, RSC Adv. 5 (2015) 70874–70882.

[51] A.E. Al-Snafi, A review on *Lagerstroemia indica*: a potential medicinal plant, IOSR J. Pharm. 9 (2019) 36–42.

[52] H.N. Qin, S.A. Graham, Lagerstroemia. Flora of China, vol. 13, 2007, pp. 277–281. http://www.efloras.org.

[53] R.M. Labib, N.A. Ayoub, A.B. Singab, M.M. Al-Azizi, A. Sleem, Chemical constituents and pharmacological studies of *Lagerstroemia indica*, Phytopharmacology 4 (2013) 373–389.

[54] Y. Diab, K. Atalla, K. Elbanna, Antimicrobial screening of some Egyptian plants and active flavones from *Lagerstroemia indica* leaves, Drug. Discov. Ther. 6 (2012) 212–217.

[55] K. Xiang-mi, C. Xue-jing, C. Mei-fang, K. Wenyi, Antioxidant activity of *Lagerstroemia indica* flower, Natural Product Research and Development 2 (2015) 264–266.

[56] S.A. Elsawi, H.F. Aly, M.M. Elbatanony, A.A. Maamoun, D.M. Mowawad, Phytochemical evaluation of *Lagerstroemia indica* (L.) Pers. leaves as Anti-Alzheimer's, J. Mater. Environ. Sci. 9 (2018) 2575–2586.

[57] K.W. Woo, W.S. Suh, L. Subedi, S.Y. Kim, S.U. Choi, K.H. Kim, K.R. Lee, Phenolic derivatives from the stems of *Lagerstroemia indica* and their biological activity, Heterocycles. 91 (2015) 2355–2366.

[58] H.J. Kim, I.S. Lee, U.J. Youn, Q.C. Chen, T.M. Ngoc, D.T. Ha, H. Liu, B.S. Min, J.Y. Lee, R.S. Seong, K.H. Bae, Biphenyl quinolizidine alkaloids from *Lagerstroemia indica*, J. Nat. Prod. 72 (2009) 749–752.

[59] B. Hosnedlova, D. Kabanov, M.B. Kepinska, V.H. Narayanan, A.A. Parikesit, C. Fernandez, G. Bjørklund, H.V. Nguyen, A. Farid, J. Sochor, A. Pholosi, M. Baron, M. Jakubek, R. Kizek, Effect of biosynthesized silver nanoparticles on bacterial biofilm changes in *S. aureus* and *E. coli*, Nanomaterials 12 (2022) 2183, https://doi.org/10.3390/nano12132183.

[60] A. Behera, S. Awasthi, Anticancer, antimicrobial and hemolytic assessment of zinc oxide nanoparticles synthesized from *Lagerstroemia indica*, BioNanoSci 11 (2021) 1030–1048.

[61] Z. Alhalili, Green synthesis of copper oxide nanoparticles CuO NPs from *Eucalyptus globoulus* leaf extract: adsorption and design of experiment, Arab. J. Chem. 15 (2022) 103739, https://doi.org/10.1016/j.arabjc.2022.103739.

[62] M. Ghaedi, A.M. Ghaedi, E. Negintaji, A. Ansari, F. Mohammadi, Artificial neural network – imperialist competitive algorithm-based optimization for removal of sunset yellow using Zn $(OH)_2$ nanoparticles-activated carbon, J. Ind. Eng. Chem. 20 (2014) 4332–4343.

[63] United States Environmental Protection Agency (USEPA), Ecological Effects Test Guidelines (OPPTS 850.4200): Seed Germination/root Elongation Toxicity Test, 1996. Washington, DC, EPA 712-C-96-132, https://www.epa.gov/sites/production/files/2015-07/documents/850-1800.pdf. (Accessed 15 January 2018).

[64] S. Sukumar, A. Rudrasenan, D.P. Nambiar, Green-Synthesized rice-shaped copper oxide nanoparticles using *Caesalpinia bonducella* seed extract and their applications, ACS Omega 5 (2) (2020) 1040–1051.

[65] S. Suganya, M. Jothibas, A. Muthuvel, Effect of temperature on different properties of ZnS nanoparticles synthesized by solid-state reaction method, J. Nanosci. Nanotechnol. 4 (2019) 787–790.

[66] F. Mendiburu, Agricolae: statistical procedures for agricultural research, R package version 1.1–4 (2013). Available online: https://CRAN.R-project.org/package=agricolae. (Accessed 5 June 2021).

[67] R.R. Pillai, P.B. Sreelekshmi, A.P. Meera, Enhanced biological performance of green synthesized copper oxide nanoparticles using *Pimenta dioica* leaf extract, Mater. Today: Proc. 50 (2022) 163–172.

[68] Y. Yang, D. Xu, Q. Wu, P. Diao, Cu_2O/CuO bilayered composite as a high-efficiency photocathode for photoelectrochemical hydrogen evolution reaction, Sci. Rep. 6 (2016) 35158.

[69] F. Mafune, J.Y. Kohno, Y. Takeda, T. Kondow, H. Sawabe, Formation and size control of silver nanoparticles by laser ablation in aqueous solution, J. Phys. Chem. B 104 (2000) 9111–9117.

[70] S. Tabrez, A.U. Khan, A.A. Mirza, M. Suhail, N.R. Jabir, T.A. Zughaibi, M. Alam, Biosynthesis of copper oxide nanoparticles and its therapeutic efficacy against colon cancer, Nanotechnol. Rev. 11 (2022) 1322–1331.

[71] F. Buazar, S. Sajjad, B. Mohammad, K. Feisal, Biofabrication of highly pure copper oxide nanoparticles using wheat seed extract and their catalytic activity: a mechanistic approach, Green Process. Synth. 8 (2019) 691–702.

[72] A.Y. Ghidan, T.M. Al-Antary, A.M. Awwad, Green synthesis of copper oxide nanoparticles using *Punica granatum* peels extract: effect on green peach aphid, Environ. Nanotechnol. Monit. Manag. 6 (2016) 95–98.

[73] B. Salopek, D. Krasic, S. Filipovic, Measurement and application of zeta-potential, Rudarsko-Geolosko-Naftni Zb. 4 (1992) 147.

[74] L. Xie, Y. Li, W. Cheng, Green fabrication of copper oxide nanoparticles by *Tragopogon collinus* leaf extract: characterization and exploring their selective anticancer effects against human leukemia cell line, J. Drug Deliv. Sci. Technol. 72 (2022) 103342.

[75] M. Ali, B. Kim, K.D. Belfield, D. Norman, M. Brennan, G.S. Ali, Green synthesis and characterization of silver nanoparticles using *Artemisia absinthium* aqueous extract—a comprehensive study, Mater. Sci. Eng. C 58 (2016) 359–365, https://doi.org/10.1016/j.msec.2015.08.045.

[76] S.H. Bhuiyan, M.Y. Miah, S.C. Paul, T.D. Aka, O. Saha, M. Rahaman, J.I. Sharif, O. Habiba, M. Ashaduzzaman, Green synthesis of iron oxide nanoparticle using *Carica papaya* leaf extract: application for photocatalytic degradation of remazol yellow RR dye and antibacterial activity, Heliyon 6 (2020) e04603, https://doi.org/10.1016/j.heliyon.2020.e04603.

[77] S. Vasantharaj, S. Sathiyavimal, M. Saravanan, P. Senthilkumar, K. Gnanasekaran, M. Shanmugavel, E. Manikandan, A. Pugazhendhi, Synthesis of ecofriendly copper oxide nanoparticles for fabrication over textile fabrics: characterization of antibacterial activity and dye degradation potential, J. Photochem. Photobiol., B 191 (2019) 143–149.

[78] K. Yang, Y. Yan, H. Wang, Z. Sun, W. Chen, H. Kang, Y. Han, W. Zahng, X. Sun, Z. Li, Monodisperse Cu/Cu_2O@C core-shell nanocomposite supported on rGO layers as an efficient catalyst derived from a Cu-based MOF/GO structure, Nanoscale 10 (2018) 17647–17655.

[79] S. Yallappa, J. Manjanna, M.A. Sindhe, N.D. Satyanarayan, S.N. Pramod, K. Nagaraja, Microwave-assisted rapid synthesis and biological evaluation of stable copper nanoparticles *using T. arjuna* bark extract, Spectrochim. Acta Mol. Biomol. Spectrosc. 110 (2013) 108–115.

[80] F. Amin, B. Khattak, A. Alotaibi, M. Qasim, I. Ahmad, R. Ullah, M. Bourhia, A. Gul, S. Zahoor, R. Ahmad, Green synthesis of copper oxide nanoparticles using *Aerva Javanica* leaf extract and their characterization and investigation of *in vitro* antimicrobial potential and cytotoxic activities, Evid. Based Complement. Alternat Med. (2021) 5589703, https://doi.org/10.1155/2021/5589703.

[81] T. Baygar, N. Sarac, A. Ugur, I.R. Karaca, Antimicrobial characteristics and biocompatibility of the surgical sutures coated with biosynthesized silver nanoparticles, Bioorg. Chem. 86 (2019) 254–258.

[82] W.W. Andualem, F.K. Sabir, E.T. Mohammed, H.H. Belay, B.A. Gonfa, Synthesis of copper oxide nanoparticles using plant leaf extract of *Catha Edulis* and its antibacterial activity, J. Nanotechnology. (2020) 2932434, https://doi.org/10.1155/2020/2932434.

[83] S. Rajeshkumar, S. Menon, S.V. Kumar, M.M. Tambuwala, H.A. Bakshi, M. Mehta, S. Satija, G. Gupta, D.K. Chellappan, L. Thangavelu, K. Dua, Antibacterial and antioxidant potential of biosynthesized copper nanoparticles mediated through *Cissus arnotiana* plant extract, J. Photochem. Photobiol. B Biol. 197 (2019) 111531.

[84] K. Ssekatawa, D.K. Byarugaba, M.K. Angwe, E.M. Wampande, F. Ejobi, E. Nxumalo, M. Maaza, J. Sackey, J.B. Kirabira, Phyto-mediated copper oxide nanoparticles for antibacterial, antioxidant and photocatalytic performances, Front. Bioeng. Biotechnol. 10 (2022) 820218, https://doi.org/10.3389/fbioe.2022.820218.

[85] S. Rajeshkumar, N.T. Nandhini, K. Manjunath, P. Sivaperumal, G.K. Prasad, S.S. Alotaibi, S.M. Roopan, Environment friendly synthesis copper oxide nanoparticles and its antioxidant, antibacterial activities using Seaweed (*Sargassum longifolium*) extract, J. Mol. Struct. 1242 (2021) 130724.

[86] Q. Lv, B. Zhang, X. Xing, Y. Zhao, R. Cai, W. Wang, Q. Gu, Biosynthesis of copper nanoparticles using *Shewanella loihica* PV-4 with antibacterial activity: novel approach and mechanisms investigation, J. Hazard Mater. 347 (2018) 141–149.

[87] J.A. Lemire, J.J. Harrison, R.J. Turner, Antimicrobial activity of metals: mechanisms, molecular targets and applications, Nat. Rev. Microbiol. 11 (2013) 371–384.

[88] A.M. Eid, A. Fouda, S.E.D. Hassan, M.F. Hamza, N.K. Alharbi, A. Elkelish, A. Alharthi, W.M. Salem, Plant-based copper oxide nanoparticles; biosynthesis, characterization, antibacterial activity, tanning wastewater treatment, and heavy metals sorption, Catalysts 13 (2023) 348, https://doi.org/10.3390/catal13020348.

[89] W.A. Hailan, K.M. Al-Anazi, M.A. Farah, M.A. Ali, A.A. Al-Kawmani, F.M. Abou-Tarboush, Reactive oxygen species-mediated cytotoxicity in liver carcinoma cells induced by silver nanoparticles biosynthesized using *Schinus molle* extract, Nanomaterials 12 (2022) 161.

[90] S.S. Beevi, M.L. Narasu, B.B. Gowda, Polyphenolics profile, antioxidant and radical scavenging activity of leaves and stem of *Raphanus sativus* L, Plant Foods Hum. Nutr. 65 (2010) 8–17.

[91] S. Rajeshkumar, S. Menon, S. Venkat Kumar, M.M. Tambuwala, H.A. Bakshi, M. Mehta, S. Satija, G. Gupta, D.K. Chellappan, L. Thangavelu, K. Dua, Antibacterial and antioxidant potential of biosynthesized copper nanoparticles mediated through *Cissus arnotiana* plant extract, J. Photochem. Photobiol. B Biol. 197 (2019) 111531, https://doi.org/10.1016/j.jphotobiol.2019.111531.

[92] J. Javanmardi, C. Stushnoff, E. Locke, J.M. Vivanco, Antioxidant activity and total phenolic content of Iranian *Ocimum* accessions, Food Chem. 83 (2003) 547–550.

[93] V.N. Koshelev, O.V. Primerova, S.V. Vorobyev, L.V. Ivanova, Synthesis, redox properties and antibacterial activity of hindered phenols linked to heterocycles, Molecules 25 (2020) 2370.

[94] M. Gioria, P. Pyšek, B.A. Osborne, Timing is everything: does early and late germination favor invasions by herbaceous alien plants? J. Plant Ecol. 11 (2018) 4–16.

[95] G. Carrera-Castaño, J. Calleja-Cabrera, M. Pernas, L. Gómez, L. Oñate-Sánchez, An updated overview on the regulation of seed germination, Plants 9 (6) (2020) 703.

[96] D. Zhang, T. Hua, F. Xiao, C. Chen, R.M. Gersberg, Y. Liu, D. Stuckey, W.J. Ng, S.K. Tan, Phytotoxicity and bioaccumulation of ZnO nanoparticles in *Schoenoplectus tabernaemontani*, Chemosphere 120 (2015) 211–219.

[97] S. Subpiramaniyam, S.C. Hong, P.I. Yi, S.H. Jang, J.M. Suh, E.S. Jung, J.S. Park, L.H. Cho, Influence of sawdust addition on the toxic effects of cadmium and copper oxide nanoparticles on *Vigna radiata* seeds, Environ. Pollut. 289 (2021) 117311.

[98] D.M.V.J. Costa, P.K. Sharma, Effect of copper oxide nanoparticles on growth, morphology, photosynthesis, and antioxidant response in *Oryza sativa*, Photosynthetica 54 (2016) 110.

[99] P.K. Tiwari, S.A.K. Shweta, V.P. Singh, S.M. Prasad, N. Ramawat, D.K. Tripathi, D.K. Chauhan, A.K. Rai, Liquid assisted pulsed laser ablation synthesized copper oxide nanoparticles (CuO-NPs) and their differential impact on rice seedlings, Ecotoxicol. Environ. Saf. 176 (2019) 321–329.

[100] I. Khaldari, M.R. Naghavi, E. Motamedi, Synthesis of green and pure copper oxide nanoparticles using two plant resources via solid-state route and their phytotoxicity assessment, RSC Adv. 11 (2021) 3346–3353.

[101] S.G. Wu, L. Huang, J. Head, D.R. Chen, I.C. Kong, Y.J. Tang, Phytotoxicity of metal oxide nanoparticles is related to both dissolved metal ions and adsorption of particles on seed surfaces, J. Petrol Environ. Biotechnol. 3 (2012) 126.

[102] K.S. Ko, I.C. Kong, Toxic effects of nanoparticles on bioluminescence activity seed germination and gene mutation, Appl. Microbiol. Biotechnol. 98 (2014) 3295–3303.

[103] P.M.G. Nair, S.H. Kim, I.M. Chung, Copper oxide nanoparticle toxicity in mung bean (*Vign aradiata* L.) seedlings: physiological and molecular level responses of in vitro grown plants, Acta, Physiol. Plantarum 36 (2014) 2947–2958.
[104] A.J. Margenot, D.A. Rippner, M.R. Dumlao, S. Nezami, P.G. Green, S.J. Parikh, A.J. McElrone, Copper oxide nanoparticle effects on root growth and hydraulic conductivity of two vegetable crops, Plant Soil 431 (2018) 333–345.
[105] N. Sreeju, A. Rufus, D. Philip, Studies on catalytic degradation of organic pollutants and anti-bacterial property using biosynthesized CuO nanostructures, J. Mol. Liq. 242 (2017) 690–700.
[106] A. Singh, N.B. Singh, I. Hussain, H. Singh, Effect of biologically synthesized copper oxide nanoparticles on metabolism and antioxidant activity to the crop plants *Solanum lycopersicum* and *Brassica oleracea* var botrytis, J. Biotechnol. 262 (2017) 11–27.
[107] S. Sathiyavimal, S. Vasantharaj, D. Bharathi, M. Saravanan, E. Manikandan, S.S. Kumar, A. Pugazhendhi, Biogenesis of copper oxide nanoparticles (CuONPs) using *Sida acuta* and their incorporation over cotton fabrics to prevent the pathogenicity of Gram-negative and Gram-positive bacteria, J. Photochem. Photobiol., B 188 (2018) 126–134.
[108] A. Muthuvel, M. Jothibas, C. Manoharan, Synthesis of copper oxide nanoparticles by chemical and biogenic methods: photocatalytic degradation and in vitro antioxidant activity, Nanotechnol. Environ. Eng. 5 (2020) 14.
[109] Z. Thammavongsy, I.P. Mercer, J.Y. Yang, Promoting proton coupled electron transfer in redox catalysts through molecular design, Chem. Commun. 55 (2019) 10342–10358.
[110] A. Sharma, R.K. Dutta, Studies on the drastic improvement of photocatalytic degradation of acid orange-74 dye by TPPO capped CuO nanoparticles in tandem with suitable electron capturing agents, RSC Adv. 5 (2015) 43815–43823.
[111] K. Selvam, G. Albasher, O. Alamri, C. Sudhakar, T. Selvankumar, S. Vijayalakshmi, L. Vennila, Enhanced photocatalytic activity of novel *Canthium coromandelicum* leaves based copper oxide nanoparticles for the degradation of textile dyes, Environ. Res. 211 (2022) 113046, https://doi.org/10.1016/j.envres.2022.113046.
[112] N. Sreeju, A. Rufus, D. Philip, Studies on catalytic degradation of organic pollutants and anti-bacterial property using biosynthesized CuO nanostructures, J. Mol. Liq. 242 (2017) 690–700, https://doi.org/10.1016/j.molliq.2017.07.077.
[113] D.B. Manikandan, M. Arumugam, S. Veeran, A. Sridhar, R.K. Sekar, B. Perumalsamy, T. Ramasamy, Biofabrication of ecofriendly copper oxide nanoparticles using *Ocimum americanum* aqueous leaf extract: analysis of in vitro antibacterial, anticancer, and photocatalytic activities, Environ. Sci. Pollut. Res. 28 (2021) 33927–33941, https://doi.org/10.1007/s11356-020-12108-w.
[114] E.S. Mehr, M. Sorbiun, A. Ramazani, S.T. Fardood, Plant-mediated synthesis of zinc oxide and copper oxide nanoparticles by using *Ferulago angulata* (schlecht) boiss extract and comparison of their photocatalytic degradation of Rhodamine B (RhB) under visible light irradiation, J. Mater. Sci. Mater. Electron. 29 (2018) 1333–1340, https://doi.org/10.1007/s10854-017-8039-3.
[115] G.K. Weldegebriel, Photocatalytic and antibacterial activity of CuO nanoparticles biosynthesized using *Verbascum thapsus* leaf extract, Optik 204 (2020) 164230, https://doi.org/10.1016/j.ijleo.2020.164230.
[116] K. Dulta, G.K. Ağçeli, P. Chauhan, R. Jasrotia, P.K. Chauhan, J.O. Ighalo, Multifunctional CuO nanoparticles with enhanced photocatalytic dye degradation and antibacterial activity, Sustain. Environ. Res. 32 (2022) 2, https://doi.org/10.1186/s42834-021-00111-w.
[117] H. Le Tu, Biosynthesis, characterization and photocatalytic activity of copper/copper oxide nanoparticles produced using aqueous extract of *Lemongrass* Leaf, Compos. Mater. 3 (2019) 30–35.
[118] H.R. Naika, K. Lingaraju, K. Manjunath, D. Kumar, G. Nagaraju, D. Suresh, H. Nagabhushana, Green synthesis of CuO nanoparticles using *Gloriosa superba* L. extract and their antibacterial activity, J. Taibah Univ. Sci. 9 (2015) 7–12, https://doi.org/10.1016/j.jtusci.2014.04.006.
[119] D. Vaidehi, V. Bhuvaneshwari, D. Bharathi, B.P. Sheetal, Antibacterial and photocatalytic activity of copper oxide nanoparticles synthesized using *Solanum lycopersicum* leaf extract, Mater. Res. Express 8 (2018) 085403, https://doi.org/10.1088/2053-1591/aad426.
[120] S. Ghosh Das, R. Ghosh, S. Dam, M. Baskey, *Madhuca longifolia* plant mediated green synthesis of cupric oxide nanoparticles: a promising environmentally sustainable material for wastewater treatment and efficient antibacterial agent, J. Photochem. Photobiol., B 189 (2018) 66–73, https://doi.org/10.1016/j.jphotobiol.2018.09.023.
[121] D. Li, Y. Liu, H. Liu, Z. Li, L. Lu, J. Liang, Z. Huang, W. Li, Nitrogen-doped carbon enhanced mesoporous TiO2 in photocatalytic remediation of organic pollutants, Res. Chem. Intermed. 46 (2020) 1065–1076, https://doi.org/10.1007/s11164-018-3531-9, 2020.
[122] G. Sorekine, G. Anduwan, M.N. Waimbo, H. Osora, S. Velusamy, S. Kim, Y.S. Kim, J. Charles, Photocatalytic studies of copper oxide nanostructures for the degradation of methylene blue under visible light, J. Mol. Struct. 1248 (2022) 131487, https://doi.org/10.1016/j.molstruc.2021.131487.
[123] A.S. Elfeky, S.S. Salem, A.S. Elzaref, M.E. Owda, H.A. Eladawy, A.M. Saeed, M.A. Awad, R.E. Abou-Zeid, A. Fouda, Multifunctional cellulose nanocrystal/metal oxide hybrid, photo-degradation, antibacterial and larvicidal activities, Carbohydr. Polym. 230 (2020) 115711.
[124] A. Fouda, S.S. Salem, A.R. Wassel, M.F. Hamza, T.I. Shaheen, Optimization of green biosynthesized visible light active CuO/ZnO Nano-photocatalysts for the degradation of organic methylene blue dye, Heliyon 6 (2020) e04896.
[125] M.T.H. van Vliet, E.R. Jones, M. Flörke, W.H.P. Franssen, N. Hanasaki, Y.J.R. Wada, Global water scarcity including surface water quality and expansions of clean water technologies, Environ. Res. Lett. 16 (2021) 024020.
[126] D. Deepa R. Keerthana, P.R. Kumar, R. Suryaprakash, Primary treatment of dairy wastewater using bio-based natural coagulants, Mater. Today (2022) 616–621.
[127] A.A. Owodunni, S. Ismail, N.G. Olaiya, Parametric study of novel plant-based seed coagulant in modeled wastewater turbidity removal, Environ. Sci. Pollut. Res. Int. (2022), https://doi.org/10.1007/s11356-022-21353-0.
[128] A. Murali, K.D. Hillstead, B.S. Wrobel, D.J. Thomas, R. Gonety, V.V. Tarabara, *Moringa oleifera*-derived coagulants for water treatment: floc structure, residual organics, and performance trade-offs, Environ. Sci. Pollut. Res. 29 (2022) 24381–24389.
[129] A.S. Taiwo, K. Adenike, O. Aderonke, Efficacy of a natural coagulant protein from *Moringa oleifera* (Lam) seeds in treatment of Opa reservoir water, Ile-Ife, Nigeria, Heliyon 6 (2020) e03335.
[130] N. Das, N. Ojha, S.K. Manda, Wastewater treatment using plant-derived bioflocculants: green chemistry approach for safe environment, Water Sci. Technol. 83 (2021) 1797–1812.
[131] J. Jumadi, A. Kamari, J.S.J. Hargreaves, N. Yusof, A review of nano-based materials used as flocculants for water treatment, Int. J. Environ. Sci. Technol. 17 (2020) 3571–3594, https://doi.org/10.1007/s13762-020-02723-y.